Journal of Dental Research
2017, Vol. 96(5) 562–570

DOI: 10.1177/0022034516685048
journals.sagepub.com/home/jdr

Endothelial Tight Junctions Are Opened in Cholinergic-Evoked Salivation In Vivo

X. Cong[1], Y. Zhang[1], Q.H. He[2], T. Wei[3], X.M. Zhang[3], J.Z. Zhang[1], R.L. Xiang[1], G.Y. Yu[3], and L.L. Wu[1]

Abstract

Blood vessels provide the original supplies for the formation of primary saliva, which is regulated by the tight junctions (TJs) between endothelial cells. Previous studies have shown that blood flow increases with vasodilatation during cholinergic-evoked salivation. However, changes in vascular paracellular permeability and the role of endothelial TJs in salivation are unknown. Here, we established an in vivo paracellular permeability detection system and observed that the endothelial TJs were permeable to 4-kDa fluorescein isothiocyanate (FITC)–dextran while impermeable to 40- and 70-kDa FITC-dextran under an unstimulated condition in mouse submandibular glands (SMGs). Pilocarpine increased the flux of 4- and 40-kDa FITC-dextran out of blood vessels but did not affect 70-kDa FITC-dextran. Claudin 5, a TJ protein specifically localized in salivary endothelial cells, was redistributed from the apicolateral membranes to the lateral and basolateral membranes and cytoplasm in cholinergic-stimulated mouse SMGs and freshly cultured human SMG tissues. In the transplanted SMGs from epiphora patients, we found that claudin 5 was present in the basolateral membranes and cytoplasm, instead of the apical region in control SMGs. Moreover, the level of phospho–myosin light chain 2 increased within the blood vessels of the pilocarpine-stimulated mouse SMGs and transplanted human SMGs, while the downstream molecule F-actin was reorganized in the endothelial cells of the transplanted human SMGs. Taken together, our findings provide direct visual evidence that the opening of endothelial TJs and the redistribution of claudin 5 are essential events contributing to cholinergic-evoked salivation, thus enriching our understanding of the secretory mechanisms that link blood flow to primary saliva formation by regulating the endothelial paracellular permeability.

Keywords: endothelium, submandibular gland, secretion, claudin 5, myosin light chains, F-actin

Introduction

Saliva is crucial for the maintenance of oral and systemic health. The secretion arises by the formation of interstitial fluid from blood vessels, which is modified and secreted into the acinar lumen and then further modified when it passes through the ductal system (Melvin et al. 2005). Among many factors that affect the production of saliva, blood flow to the salivary glands is a key factor that affects salivary secretion by supplying energy and nutrients in addition to the ions and water that form the primary fluid in acini. Since 1858, when Bernard first investigated salivary blood flow by parasympathetic innervation in cats, many studies have investigated the significance of blood flow in secretory responses. The activation of parasympathetic nerves increases salivation and causes vasodilatation, followed by an increase in blood flow (Anderson and Garrett 1998). A significant reduction in submandibular gland (SMG) blood flow and secretion occurs when blood pressure decreases by approximately 50% in cats; more important, salivary flow is linearly related to blood flow within the gland (Hanna et al. 1999). In healthy volunteers, color Doppler sonography analysis shows a significant correlation between blood flow in the SMG and salivary secretion caused by gustatory stimuli, whereas in patients with Sjögren's syndrome, blood flow in response to the secretory stimulus lemon extracts is defective in the SMG (Ariji et al. 1998; Chikui et al. 2000). These data indicate that blood flow plays a dominant role in the formation

[1]Center for Salivary Gland Diseases of Peking University School and Hospital of Stomatology, Department of Physiology and Pathophysiology, Peking University School of Basic Medical Sciences, Key Laboratory of Molecular Cardiovascular Sciences, Ministry of Education, and Beijing Key Laboratory of Cardiovascular Receptors Research, Beijing, P.R. China
[2]Center of Medical and Health Analysis, Peking University Health Science Center, Beijing, P.R. China
[3]Department of Oral and Maxillofacial Surgery, Peking University School and Hospital of Stomatology, Beijing, P.R. China

A supplemental appendix to this article is available online.

Corresponding Authors:
G.Y. Yu, Department of Oral and Maxillofacial Surgery, School and Hospital of Stomatology, Peking University, Beijing, 100081, P.R. China.
Email: gyyu@263.net
L.L. Wu, Department of Physiology and Pathophysiology, Peking University School of Basic Medical Sciences, Beijing, 100191, P.R. China.
Email: pathophy@bjmu.edu.cn

of saliva by the SMG. However, the factor that determines the transport of solutes from the blood vessels to the salivary glands is still unclear.

Endothelial cells are the innermost component of blood vessels, and tight junctions (TJs) located at the most apical portion of their lateral membranes serve as gatekeepers for the endothelial paracellular pathway (Tsukita et al. 2001; González-Mariscal et al. 2008). Previous studies have shown that the vascular endothelium is crucial for maintaining homeostasis in the ocular anterior segment (Yang et al. 2015). Treatment with fenofibric acid prevents the aberrant distribution of TJ proteins in rat retinal endothelial cells, which is a possible mechanism for reducing excessive permeability in diabetic patients (Roy et al. 2015). In addition, abnormal endothelial TJs are found in active lesions and normal-appearing white matter in multiple sclerosis (Plumb et al. 2002). These studies suggest that TJs are indispensable structures for vascular paracellular permeability. However, because it has been experimentally difficult to investigate endothelial TJs in salivary glands, especially in vivo, the exact role of endothelial TJs in regulating salivary secretion is still unknown.

Dry eye syndrome is a common ophthalmologic disease characterized by reduced or absent tears, corneal changes, and even loss of vision (Lemp et al. 2007). Transplantation of autologous SMGs into the temporal fossa with implantation of the Wharton's duct into the upper conjunctival fornix provides a continuous and endogenous supply of fluid to replace insufficient tears, which is an effective method for treating severe dry eye syndrome (Geerling et al. 1998; Yu et al. 2004). However, >40% of patients suffer from epiphora 6 mo post-transplantation, which may lead to social embarrassment, blurred vision, and even corneal edema (Yu et al. 2004; Geerling et al. 2008). Schirmer's test shows that the flow of secretion is >35 mm/5 min. The transplanted SMG has to be partly resected to reduce the secretion for patients with severe epiphora.

Therefore, the present study was designed to explore the function of salivary endothelial TJs during cholinergic stimulation by establishing an in vivo paracellular permeability detection system. Furthermore, we investigated the expression pattern of claudin 5—a cell type–specific TJ transmembrane protein expressed in endothelial cells—in mouse SMG tissues and SMGs from epiphora patients, with a possible mechanism involved in the regulation of salivary endothelial TJs.

Materials and Methods

Reagents and Antibodies

Pilocarpine, carbachol, fluorescein isothiocyanate (FITC)–labeled dextran (molecular weight: 4, 40, and 70 kDa), and FITC-labeled phalloidin were purchased from Sigma-Aldrich. Antibody to claudin 5 was purchased from Bioworld Technology; antibody to CD-31, from Origene Technologies; antibody to ZO-1 from Life Technologies; and antibodies to myosin light chain 2 (MLC2) and phospho-MLC2 (p-MLC2), from Cell Signal Technology.

Measurement of Saliva Secretion

C57BL/6 male mice (8 to 10 wk old) were obtained from the Peking University Health Science Center. All experimental procedures were approved by the Ethics Committee of Animal Research, Peking University Health Science Center, and complied with the *Guide for the Care and Use of Laboratory Animals* (publication 85-23, revised 1996; National Institutes of Health). All animal research is reported in accordance with the ARRIVE guidelines (Kilkenny et al. 2010).

Mice were fasted for a minimum of 5 h with water ad libitum. After anesthesia with an intraperitoneal injection of chloral hydrate (0.4 g/kg body weight), the SMG duct was separated and inserted into a capillary tube. After stimulation with the cholinergic agonist pilocarpine (10 μg/g, body weight, intraperitoneal), the volume was recorded every 1 min to monitor the flow rate (μL/min).

In Vivo Paracellular Permeability Assay

The effect of pilocarpine on the paracellular permeability of SMG endothelium was observed as previously described with modifications (Masedunskas et al. 2012). Briefly, 1.5 mg/g of body weight of the paracellular permeability tracer FITC-dextran (4, 40, or 70 kDa) was injected into the caudal vein; then, the right SMG was separated and placed in the glass chamber under a 2-photon laser-scanning microscope (Leica TCS SP8). Images were taken every 5 s for the areas that included blood vessels in the mesenchyma and acini in the parenchyma, while the microvessels were captured with a higher zoom every 0.133 s for faster speed and better observations before and after pilocarpine injection. For quantitative analysis, fluorescence intensities were measured with ImageJ Software (National Institutes of Health). The intensities within acini and ducts and the basal surfaces of acini were all shown as ratios of the intensity within blood vessels, which were adjusted to 1.00 under normal conditions.

Human SMG Tissue Collection and Culture

Transplanted SMG tissues were collected from 6 individuals (40 to 55 y old, 4 men) who underwent partial gland reduction for epiphora within 3 to 12 mo after transplantation. SMGs from patients who underwent functional neck dissection for primary oral squamous cell carcinoma without irradiation and chemotherapy were used as controls. All control tissues were confirmed to be histologically normal. The research was approved by the Peking University Institutional Review Board, and all patients signed an informed consent document before tissue collection. SMG tissues were cultured as previously described (Ding et al. 2014).

Transmission Electron Microscopy

SMG tissues were fixed in 2% paraformaldehyde–1.25% glutaraldehyde. Ultrathin sections were stained with uranyl acetate and lead citrate and then examined with a transmission electron microscope (Hitachi H-7000).

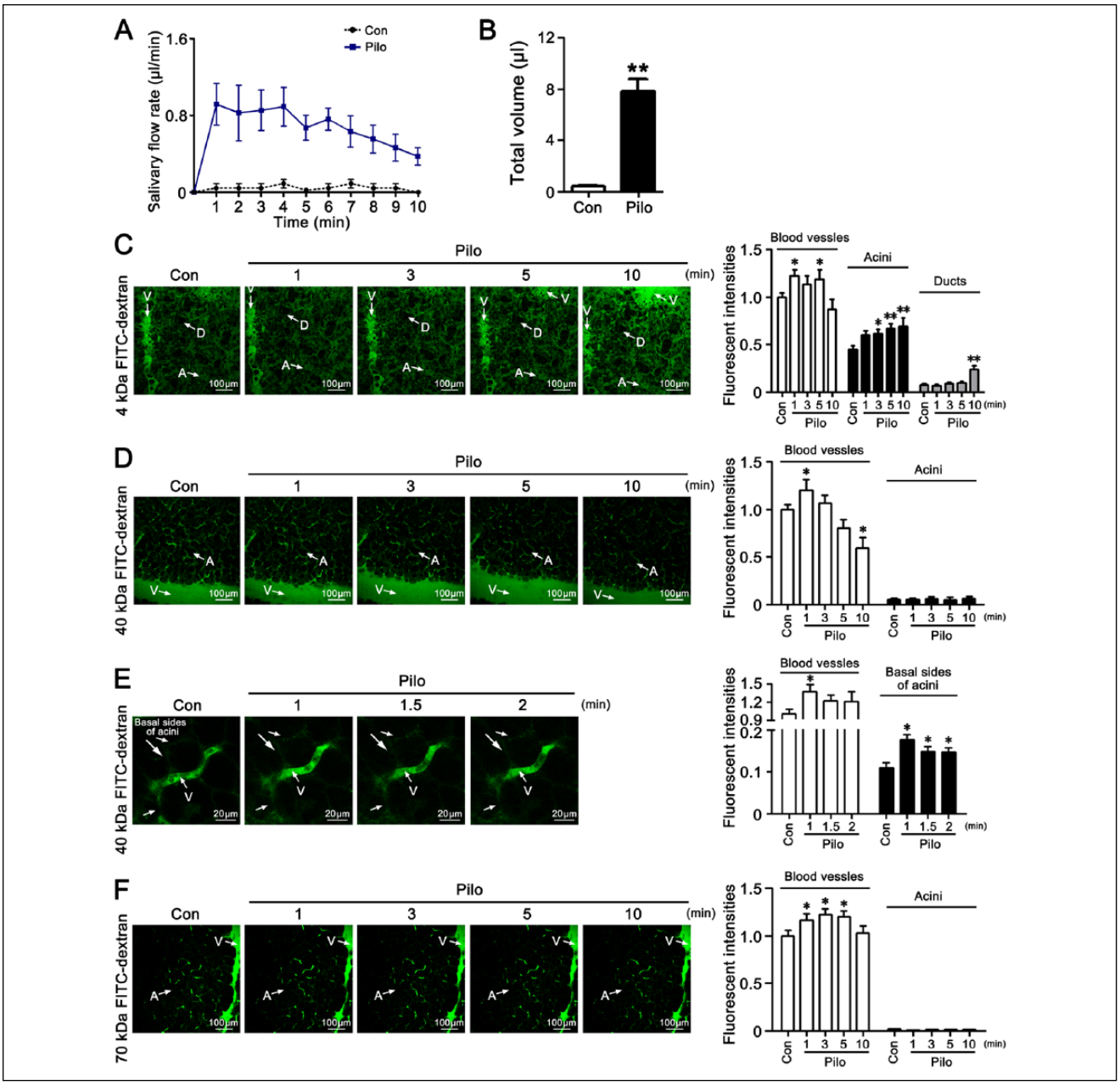

Figure 1. Effects of pilocarpine on salivary secretion and paracellular permeability in mouse in vivo. (**A**, **B**) The flow rate (A) and total volume (B) of the saliva secreted from the submandibular gland (SMG) were collected for 10 min after pilocarpine stimulation (10 μg/g, body weight, intraperitoneal). (**C**–**F**) The paracellular permeability assay in vivo was performed by injecting 4-, 40-, or 70-kDa fluorescein isothiocyanate (FITC)–dextran into the caudal vein (1.5 mg/g, body weight) and then separating the right SMG and placing it on a glass chamber under a 2-photon laser-scanning microscope. Left: white arrows indicate the structures of the SMG. For the areas including blood vessels in the mesenchyma and acini in the parenchyma, images were taken every 5 s for 10 min, and representative images at 1, 3, 5, and 10 min after pilocarpine stimulation and control are shown on the left (bars: 100 μm). For areas including microvessels under higher zoom, images were captured every 0.133 s for 2 min, and representative images at 1, 1.5, and 2 min after pilocarpine stimulation and control are shown (bars: 20 μm). Right: for quantitative analysis, the fluorescence intensity was measured by the ImageJ Software. The fluorescence intensities within blood vessels, acini, ducts, and the basal sides surrounding acini are shown as the relative ratios of the intensity within blood vessels in unstimulated control conditions. All data are presented as mean ± SEM from the results of 6 independent experiments. *$P < 0.05$ and **$P < 0.01$, compared with controls. A, acinus; con, control; D, duct; pilo, pilocarpine; V, vessel.

Histologic and Immunofluorescence Staining

Paraffin or frozen sections of SMGs were stained with hematoxylin and eosin, and morphologic changes were observed under a light microscope (Leica Q550CW). SMG tissue sections (6 μm) were fixed in cold acetone, blocked with 1% bovine serum albumin, stained with primary antibodies at 4 °C overnight, and then incubated with Alexa Fluor 594– and/or

488–conjugated secondary antibodies at 37 °C for 2 h. Nuclei were stained with 4′,6-diamidino-2-phenylindole. Fluorescence images were captured with a confocal microscope (Leica TCS SP8), and representative images of cylindrical blood vessels were shown simultaneously in 1 section.

Statistical Analysis

Data are shown as mean ± SEM. Statistical analysis was performed with a Student's *t* test for 2 groups or an analysis of variance with multiple groups. $P < 0.05$ was considered statistically significant.

Results

Effect of Pilocarpine on Salivary Endothelial Paracellular Permeability In Vivo

Stimulation with pilocarpine rapidly induced salivary secretion in mice, as shown by significant increases in secretory flow rate and the total volume of secreted saliva in 10 min (Fig. 1A, B).

The function of endothelial TJs was detected with different molecular weights of FITC-dextran. Under unstimulated conditions, 4-kDa FITC-dextran was not only found within blood vessels but also distributed around the basolateral and apical sides of acini, while the lumen of the ducts contained less fluorescence. After pilocarpine stimulation, the fluorescence intensity within blood vessels obviously increased at 1, 3, and 5 min and then declined at 10 min. Meanwhile, the fluorescence intensity within acinar islets significantly increased and lasted for 10 min, and the fluorescence intensity in the lumen of ducts slightly increased at 10 min (Fig. 1C; Appendix Movies 1, 2). Under unstimulated conditions, 40-kDa FITC-dextran was mainly localized in blood vessels and microvessels, and the fluorescence intensity increased at 1 min while gradually decreased at 5 and 10 min after pilocarpine stimulation. However, the fluorescence intensity of 40-kDa FITC-dextran within acini did not change significantly in response to pilocarpine (Fig. 1D; Appendix Movies 3, 4). We further used faster speed and higher zoom to trace the flux of tracers

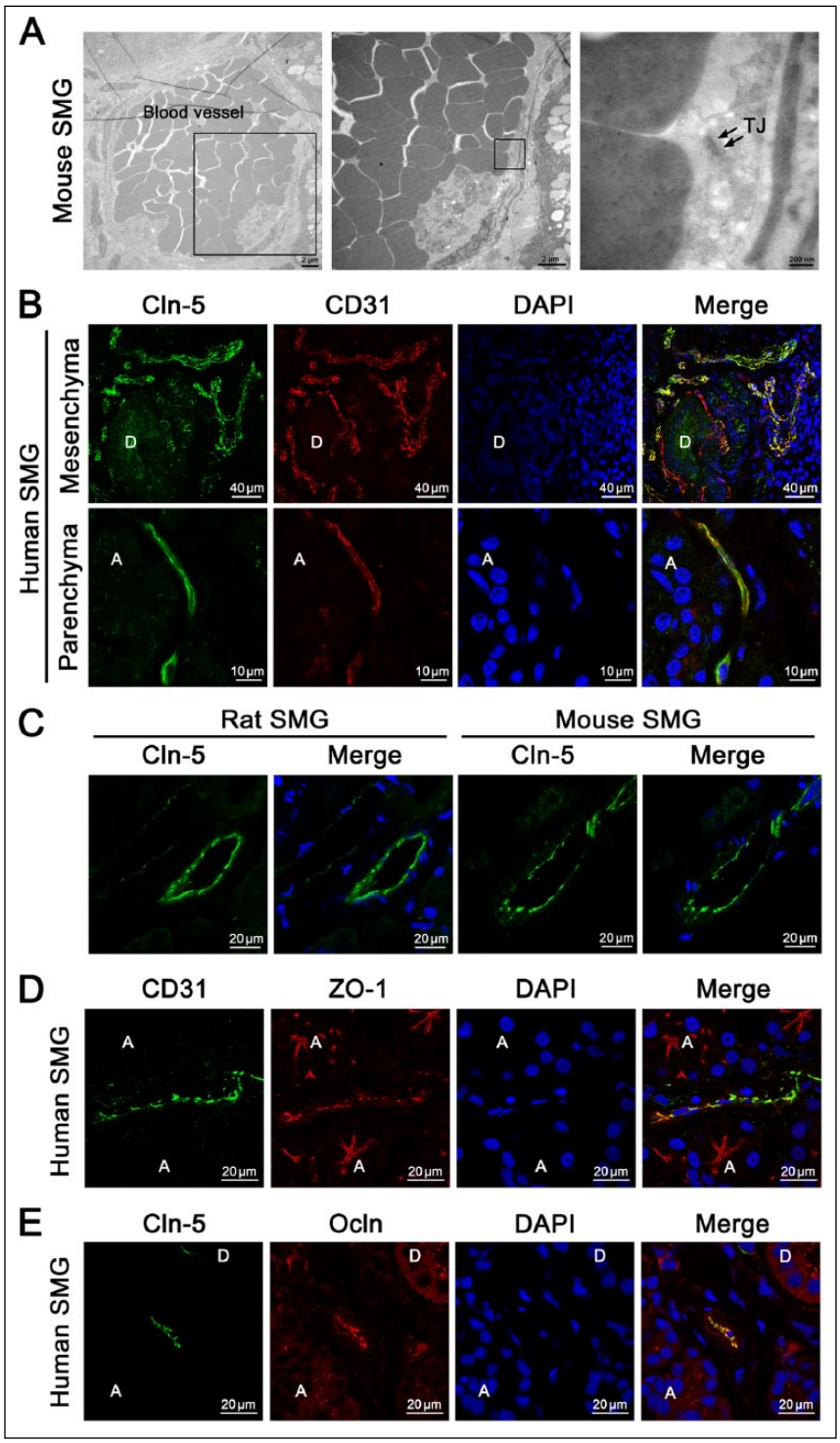

Figure 2. Assessment of the endothelial tight junction (TJ) ultrastructure and the distribution pattern of claudin 5 (Cln-5) in the submandibular gland (SMG). (**A**) Ultrastructure images of the endothelial TJ in mouse SMG were observed under a transmission electron microscope. Boxed areas are shown at higher magnifications in the right panels. Arrows show TJs between neighboring endothelial cells in blood vessels of mouse SMG. Bars: 2 μm and 200 nm (as indicated). (**B**) Coimmunostaining of Cln-5 with the endothelial cell marker CD31 in human SMGs. Areas in the mesenchyma and parenchyma of SMGs were observed. Cell nuclei were stained with DAPI (blue). Bars: 40 μm and 10 μm for the upper and lower panels, respectively. (**C**) The distribution of Cln-5 in rat SMG (left) and mouse SMG (right). Bars: 20 μm. (**D**, **E**) Coimmunostaining of CD31 and ZO-1 (D) and Cln-5 and occludin (E) in human SMG. Bars: 20 μm. A, acinus; D, duct; Ocln, occludin.

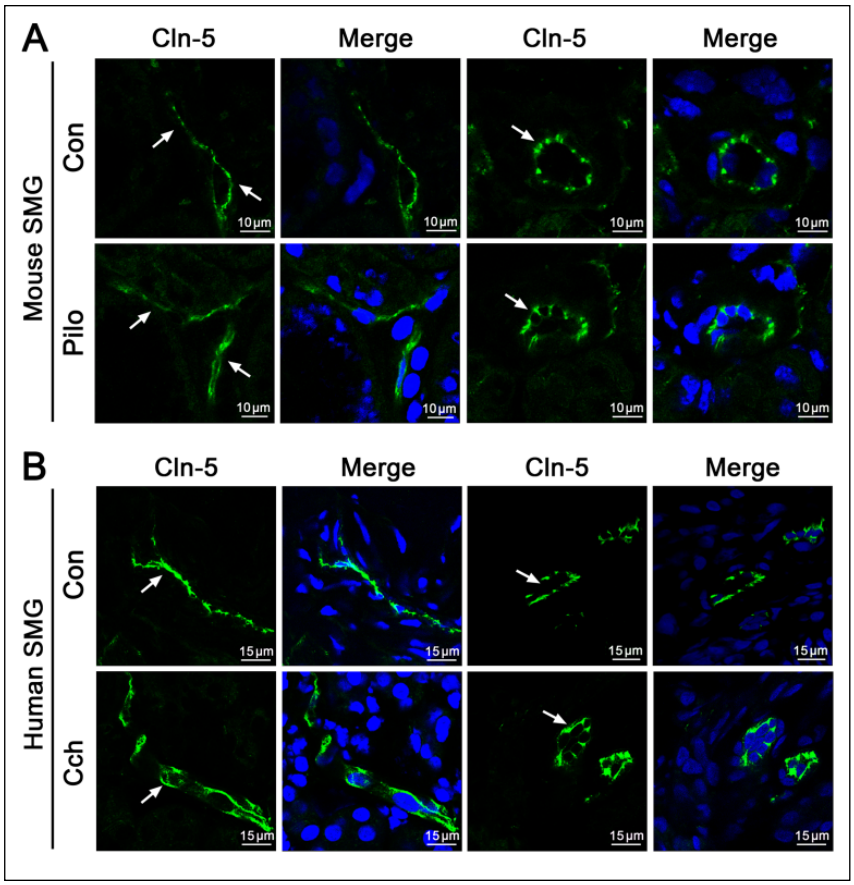

Figure 3. Changes in claudin 5 (Cln-5) distribution in the submandibular gland (SMG) by cholinergic stimulation in vivo and in vitro. (**A**) SMGs were harvested from control (con) and pilocarpine (pilo)–stimulated mouse models. The immunofluorescence images of Cln-5 were taken with a confocal microscope, and the microvessels are displayed in 2 planes. Bars: 10 μm. (**B**) Human SMG tissues were incubated with carbachol (Cch; 10 μmol/L) for 5 min. The distribution of Cln-5 staining and images of the microvessels are displayed in 2 different planes. Bars: 15 μm. White arrows indicated changes in Cln-5 distribution in SMGs.

in the microvessels and found that the fluorescence intensity at the basal sides surrounding acini increased by pilocarpine (Fig. 1E). In contrast, the largest tracer, 70-kDa FITC-dextran, predominantly existed in blood vessels with little fluorescence observed in the acini of unstimulated SMGs. Stimulation with pilocarpine increased the fluorescence intensity of 70-kDa FITC-dextran within vessels at 1, 3, and 5 min; fluorescence intensity then returned to control levels, while no obvious flux of tracer was found within acini (Fig. 1F; Appendix Movies 5, 6).

Expression Pattern of Claudin 5 in SMGs

In the endothelium, TJs serve as gatekeepers to modulate the movement of solutes and proteins from blood vessels to the surrounding tissues. By transmission electron microscopy, the average distance between neighboring endothelial TJs in mouse SMGs was 34.89 nm (Fig. 2A).

Claudin 5 is a TJ transmembrane protein that is particularly expressed in endothelial cells, as previously reported (Peppi and Ghabriel 2004). We detected the expression pattern of claudin 5 in human, rat, and mouse SMG tissues. In the mesenchymal area of human SMGs where there were many large blood vessels around the striated ducts, claudin 5 localized to the innermost sides of neighboring endothelial cells and co-localized with CD31, an endothelial cell marker. In the parenchyma of human SMGs, claudin 5 was expressed in the microvessels surrounding acini, as evidenced by its colocalization with CD31 (Fig. 2B). In rat and mouse SMGs, claudin 5 showed a similar distribution pattern (Fig. 2C). In addition, the TJ cytoplasm protein ZO-1 and the TJ transmembrane protein occludin were also expressed in the endothelial cells, while they were more ubiquitously distributed at the apicolateral membranes of acini and ducts in human SMGs (Fig. 2D, E).

Alterations in Claudin 5 Distribution in Response to Cholinergic Stimulation

Since claudin 5 was the primary specific TJ component in salivary endothelium, we investigated changes in claudin 5 in vivo and in vitro. Mouse acinar and ductal cells, as well as blood vessels, were observed in unstimulated SMGs by light microscopy, while they did not change after pilocarpine stimulation (Appendix Fig. 1A). The most apically expressed claudin 5 was redistributed to the basolateral membranes and dispersed into the cytoplasm in SMGs, as shown in 2 vessel planes (Fig. 3A). To determine whether this change was the direct effect of cholinergic stimulation, we cultured freshly isolated human SMG tissues. Carbachol induced claudin 5 relocation from the apical portion of endothelial cells to the basolateral membrane and cytoplasm at 5 min (Fig. 3B), while the gland morphology remained the same in SMG tissues with or without carbachol treatment (Appendix Fig. 1B). Under unstimulated conditions, claudin 5 was co-localized with ZO-1 and occludin but not Na^+-K^+-ATPase, which is expressed in the basolateral membranes of endothelial and acinar cells. After pilocarpine stimulation, a more extended expression of claudin 5 than that of ZO-1 and occludin as well as a partial co-localization of claudin 5 with the Na^+-K^+-ATPase was observed, suggesting that claudin 5 was partially relocated from the apicolateral membranes to the basolateral membranes in vivo (Appendix Fig. 2). These results suggest that activation of muscarinic acetylcholine receptor induces claudin 5 redistribution with a concomitant increase in salivary secretion, and this alteration might contribute to the endothelial TJ opening induced by cholinergic stimulation.

Alterations in Claudin 5 Distribution in SMGs from Epiphora Patients

Next, we explored whether the alteration of endothelial TJs occurred in SMGs from epiphora patients who had received SMG autotransplantation surgery and subsequently received partial gland reduction due to severe epiphora. Compared with the control SMGs obtained from patients who received functional neck dissection, the acinar area was decreased, while the blood vessels and microvessels were not significantly changed in the transplanted SMG tissues (Appendix Fig. 1C). However, in the transplanted SMGs, claudin 5 was not only localized to the most apical portion of the neighboring endothelial cells but also expressed in the lateral membranes and the cytoplasm of the endothelial cells (Fig. 4A). This further indicates that the changes in claudin 5 distribution might be involved in altered secretion in the transplanted SMGs.

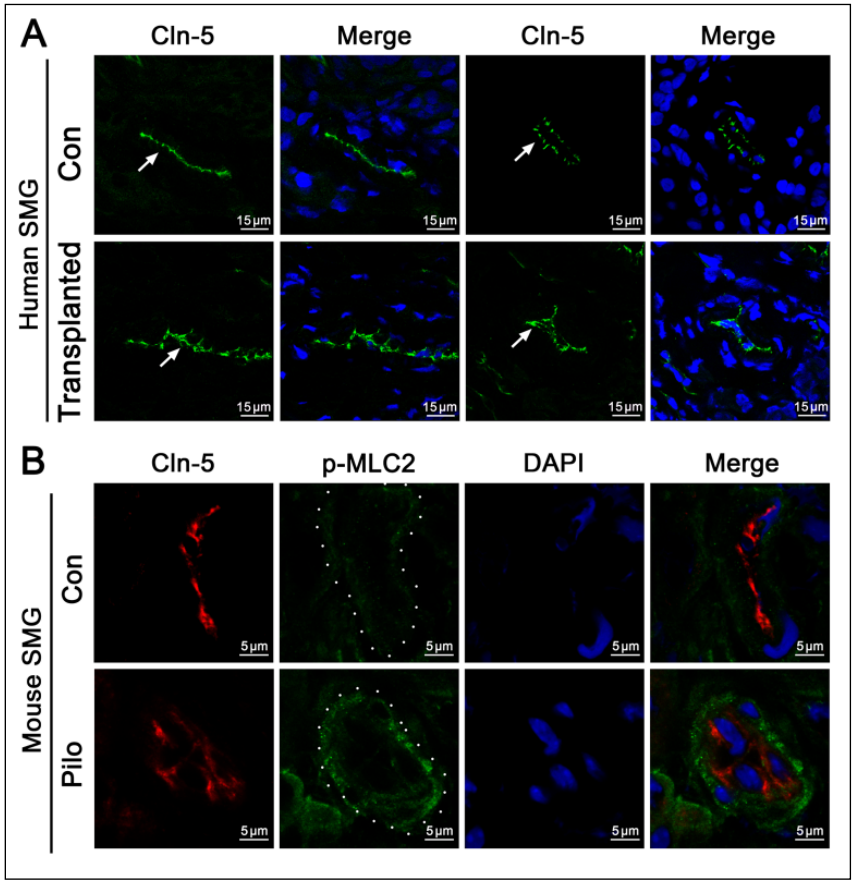

Figure 4. Changes in claudin 5 (Cln-5) distribution in submandibular glands (SMGs) from epiphora patients, and changes in Cln-5 and phospho-myosin light chain 2 (p-MLC2) distribution by cholinergic stimulation in vivo. (**A**) The distribution of Cln-5 in the SMGs from control (con) and transplanted human SMGs. The transplanted SMGs were collected from epiphora patients who underwent partial gland reduction after transplantation, while the control glands were from patients who underwent functional neck dissection for primary oral squamous cell carcinoma without irradiation and chemotherapy. The immunofluorescence images of Cln-5 were taken with a confocal microscope, and the microvessels are displayed in 2 different planes. Bars: 15 μm. White arrows indicated changes in Cln-5 distribution in SMGs. (**B**) Coimmunostaining of Cln-5 and p-MLC2 in control and pilocarpine (pilo)–stimulated mouse SMGs. Bars: 5 μm. White dots indicate the edges of blood vessels.

Changes in the MLC2/F-actin Signaling Pathway in Transplanted SMGs

We further explored mechanisms that could modulate the endothelial TJs in SMGs. The phosphorylation of MLC2 has been reported to play a crucial role in regulating the distribution of TJs, mainly through altering the organization of cytoskeletal F-actin, which directly links with TJs (Hecht et al. 1996; Shen et al. 2006; Cong et al. 2012, Cong et al. 2013). The specificity of the p-MLC2 antibody was confirmed with Western blotting in 2 cultured endothelial cells (Appendix Fig. 3). Using coimmunofluorescence staining, we observed that the expression level of p-MLC2 was low in blood vessels in control SMGs, whereas it was obviously elevated when claudin 5 was redistributed toward the basolateral membranes of endothelial cells in the SMGs of the pilocarpine-stimulated mouse model (Fig. 4B). Similar results were also seen in the transplanted SMGs of epiphora patients, with increased levels of p-MLC2 observed in blood vessels (Fig. 5A). Moreover, we observed the organization of F-actin in the transplanted SMGs obtained from epiphora patients. In control glands, F-actin was distributed in the periapical portion of neighboring endothelial cells and was partially co-localized with claudin 5. However, in the transplanted SMGs, F-actin was dispersed into the cytoplasm in parallel with the claudin 5 redistribution (Fig. 5B). In addition, the fluorescence intensities of F-actin in the apical and lateral cytoplasm of acini were decreased in the transplanted glands (Fig. 5C).

Discussion

In the present study, using an in vivo detection system, we identified that the endothelial paracellular permeability of SMGs increased with an accompanying increase in salivation and that the redistribution of claudin 5 from the apicolateral membranes to the lateral and basolateral membranes and cytoplasm was responsible for the endothelial TJs opening. Moreover, the MLC2/F-actin signaling pathway may be involved in regulation of endothelial TJs in the SMG. These results indicate that the opening of endothelial TJs might be a prerequisite for salivary secretion and that claudin 5 is a potential target for modulating salivation through regulation of the paracellular permeability of blood vessels.

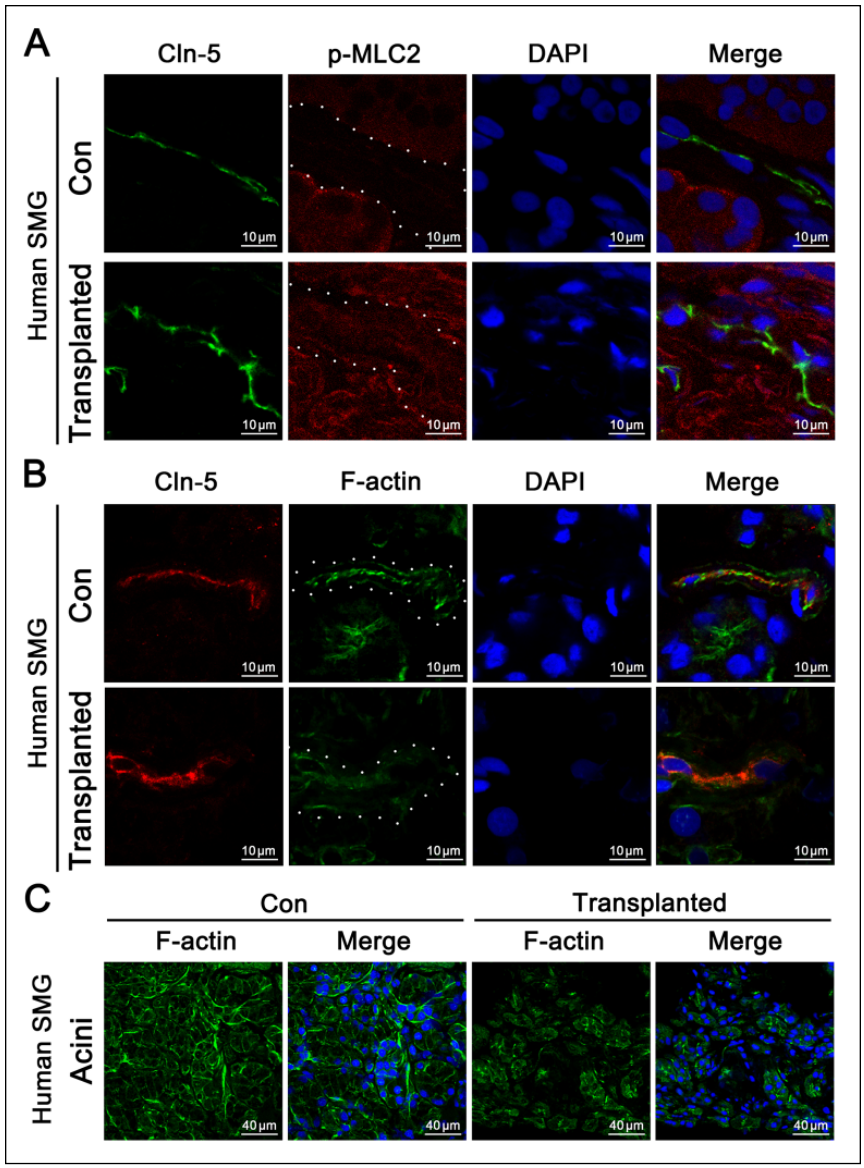

Figure 5. Changes in coimmunostaining of claudin 5 (Cln-5) and phospho-myosin light chain 2 (p-MLC2) or F-actin in submandibular glands (SMGs) from epiphora patients. (**A**) Coimmunostaining of Cln-5 and p-MLC2 in control (Con) and transplanted human SMGs. Bars: 10 μm. White dots indicate the edges of blood vessels. (**B**) Coimmunostaining of Cln-5 with F-actin in control and transplanted human SMGs. Bars: 10 μm. White dots indicate the edges of blood vessels. (**C**) The distribution of F-actin in acini of control and transplanted human SMGs. Bars: 40 μm.

Sufficient blood flow and normal function of blood vessels are fundamental factors that affect salivation. However, it was unclear what regulates the transport of fluid and solutes from blood vessel across the blood endothelium and then into the acinar lumen. TJs are cell-cell interactions that serve as gatekeepers to regulate transport through the paracellular pathway; however, the role of TJs in the salivary endothelium was still unknown. In the present study, we observed the ultrastructure of endothelial TJs in mouse SMGs and found that the average endothelial TJ width (34.89 nm) was larger than that of acinar and ductal cells (12.77 nm and 9.32 nm, respectively) as reported previously (Zhang et al. 2016), suggesting that the endothelial TJs are opened to a greater extent and are much more permeable than acinar and ductal cells in SMGs under unstimulated conditions. In the in vivo paracellular permeability assay, we used different molecular weights of FITC-dextran to evaluate the size of the endothelial TJ "pore." Our results showed that salivary endothelial TJs could allow small particles, such as 4-kDa FITC-dextran, to leak from blood vessels into acini and ducts but that they are less permeable or even impermeable to larger particles, such as 40- and 70-kDa FITC-dextran, under unstimulated conditions, suggesting that the extent of the TJ opening in salivary endothelium is <40-kDa FITC-dextran in unstimulated mouse SMGs. Cholinergic stimulation by pilocarpine significantly enhanced the flux of 4-kDa FITC-dextran into acini and ducts, and 40-kDa FITC-dextran diffused to the basal sides of acini, although the latter was unable to enter into the lumen of acini because of the tighter TJs in acinar cells than endothelial cells. In contrast, 70-kDa FITC-dextran was unable to cross the salivary microvessels. Meanwhile, the fluorescence intensities of the tracers in blood vessels were increased due to increased blood flow and vasodilatation as reported previously (Anderson and Garrett 1998). Our previous study determined that activation of muscarinic acetylcholine receptor modulates TJ proteins in the SMG acinar epithelium (Cong et al. 2015). Here, our in vivo data provide direct visual evidence that cholinergic stimulation induces the opening of TJs in the SMG endothelium, which then supplies the prerequisites to produce primary saliva in acini. Our findings imply that there is an important link between the opening of endothelial and acinar epithelial TJs during salivation.

Among the different types of TJ proteins, claudin 5 is known as an important and indispensable TJ transmembrane protein in endothelial cells. In claudin 5–deficient mice, the permeability of the blood-brain barrier is profoundly increased, which leads to death within a few hours of birth (Nitta et al. 2003). Adrenomedullin secreted by brain vascular endothelial cells inhibits paracellular transport in brain microvascular endothelial cells through overexpression of claudin 5 (Honda et al. 2006). Claudin 5 also controls the intercellular barriers of

human dermal microvascular endothelial cells (Kluger et al. 2013). Although claudin 5 has been found to specifically localize in the blood vessel endothelium of rat SMGs (Peppi and Ghabriel 2004), there are few data regarding its role in the regulation of salivary endothelial paracellular permeability. Here, using coimmunostaining, we identified that claudin 5 is specifically expressed in the apical portion of the lateral membranes of endothelial cells in SMGs. In the pilocarpine-stimulated mouse model, claudin 5 was redistributed to the lateral and basolateral membranes and even into the cytoplasm. Similar results were found in freshly cultured human SMG tissues treated with carbachol. In the transplanted SMGs from epiphora patients, claudin 5 was removed from the apical membranes and redistributed to the lateral and basolateral membranes and cytoplasm. These results suggest that the redistribution of claudin 5 in SMG endothelium might affect the integrity of the TJ complex, thereby increasing endothelial paracellular permeability and saliva secretion.

Furthermore, we explored a possible mechanism that could modulate endothelial TJs in the SMG vascular endothelium. Phosphorylation of MLC2 is reported to alter TJ distribution by changing the organization of F-actin (González-Mariscal et al. 2008). Thrombin increases endothelial permeability in an MLC2-mediated mechanism (Garcia et al. 1995; Shi et al. 1998). Nafamostat mesylate, a synthetic serine protease inhibitor, preserves the integrity of the blood-brain barrier and alleviates changes in TJ protein expression and localization and cytoskeletal rearrangements by inhibiting of thrombin, which is correlated with regulation of the MLC2 signaling pathway (Wang et al. 2016). Hypoxia and low-glucose treatment increase MLC2 phosphorylation in rat brain microvascular endothelial cells (Yang et al. 2016). Here, we identified that the intensity of p-MLC2 within blood vessels is enhanced in pilocarpine-stimulated mouse SMGs. In human transplanted SMGs, the level of p-MLC2 in endothelial cells increased; moreover, F-actin was rearranged from the periapical region into the cytoplasm. These results indicate that changes in the redistribution of MLC2 and F-actin might be related to the increased paracellular permeability through regulation of the TJ distribution. However, more efforts with additional approaches should be made in the future to confirm the direct involvement of the MLC2/F-actin pathway in SMG endothelium. Besides, the secretion of SMG is much more than that of the lacrimal gland. Although >40% of patients suffer from epiphora 6 mo posttransplantation, we still need more evidence to evaluate whether the hypersecretory phenomenon was intrinsic to the transplanted human SMG tissue. This limitation in our study needs to be further investigated.

In summary, we demonstrate that cholinergic stimulation induces the opening of TJs in SMG endothelium and the redistribution of claudin 5, which is accompanied by increased salivation. The MLC2/F-actin signaling pathway may be responsible for modulating endothelial TJs in SMGs. Our findings provide new insights into secretory mechanisms that are important for increased vascular endothelial paracellular permeability and acinar production of primary saliva in cholinergic-stimulated salivation.

Author Contributions

X. Cong, contributed to conception, design, and data acquisition, drafted and critically revised the manuscript; Y. Zhang, contributed to design, data analysis, and interpretation, critically revised the manuscript; Q.H. He, contributed to design and data acquisition, critically revised the manuscript; T. Wei, X.M. Zhang, contributed to data acquisition, critically revised the manuscript; J.Z. Zhang, R.L. Xiang, contributed to data acquisition, drafted the manuscript; G.Y. Yu, L.L. Wu, contributed to conception, design, and data interpretation, critically revised the manuscript. All authors gave final approval and agree to be accountable for all aspects of the work.

Acknowledgments

We thank Prof. Guo-He Zhang from the National Institute of Dental and Craniofacial Research, National Institutes of Health, for providing thoughtful suggestion. This study was supported by the National Natural Science Foundation of China (grants 81300893 and 81470756), and X. Cong was supported by the Leading Academic Discipline Project of Beijing Education Bureau (grant BMU20110254) and the Youth Talent Support Program from the China Association for Science and Technology. The authors declare no potential conflicts of interest with respect to the authorship and/or publication of this article.

References

Anderson LC, Garrett JR. 1998. Neural regulation of blood flow in the rat submandibular gland. Eur J Morphol. 36 Suppl:213–218.

Ariji Y, Yuasa H, Ariji E. 1998. High-frequency color doppler sonography of the submandibular gland: relationship between salivary secretion and blood flow. Oral Surg Oral Med Oral Pathol Oral Radiol Endod. 86(4):476–481.

Chikui T, Yonetsu K, Izumi M, Eguchi K, Nakamura T. 2000. Abnormal blood flow to the submandibular glands of patients with Sjögren's syndrome: Doppler waveform analysis. J Rheumatol. 27(5):1222–1228.

Cong X, Zhang Y, Li J, Mei M, Ding C, Xiang RL, Zhang LW, Wang Y, Wu LL, Yu GY. 2015. Claudin-4 is required for modulation of paracellular permeability by muscarinic acetylcholine receptor in epithelial cells. J Cell Sci. 128(12):2271–2286.

Cong X, Zhang Y, Shi L, Yang NY, Ding C, Li J, Ding QW, Su YC, Xiang RL, Wu LL, et al. 2012. Activation of transient receptor potential vanilloid subtype 1 increases expression and permeability of tight junction in normal and hyposecretory submandibular gland. Lab Invest. 92(5):753–768.

Cong X, Zhang Y, Yang NY, Li J, Ding C, Ding QW, Su YC, Mei M, Guo XH, Wu LL, et al. 2013. Occludin is required for TRPV1-modulated paracellular permeability in the submandibular gland. J Cell Sci. 126(Pt 5):1109–1121.

Ding C, Cong X, Zhang Y, Yang NY, Li SL, Wu LL, Yu GY. 2014. Hypersensitive mAChRs are involved in the epiphora of transplanted glands. J Dent Res. 93(3):306–312.

Garcia JG, Davis HW, Patterson CE. 1995. Regulation of endothelial cell gap formation and barrier dysfunction: role of myosin light chain phosphorylation. J Cell Physiol. 163(3):510–522.

Geerling G, Garrett JR, Paterson KL, Sieg P, Collin JR, Carpenter GH, Hakim SG, Lauer I, Proctor GB. 2008. Innervation and secretory function of transplanted human submandibular salivary glands. Transplantation. 85(1):135–140.

Geerling G, Sieg P, Bastian GO, Laqua H. 1998. Transplantation of the autologous submandibular gland for most severe cases of keratoconjunctivitis sicca. Ophthalmology. 105(2):327–335.

González-Mariscal L, Tapia R, Chamorro D. 2008. Crosstalk of tight junction components with signaling pathways. Biochim Biophys Acta. 1778(3):729–756.

Hanna SJ, Brelen ME, Edwards AV. 1999. Effects of reducing submandibular blood flow on secretory responses to parasympathetic stimulation in anaesthetized cats. Exp Physiol. 84(4):677–687.

Hecht G, Pestic L, Nikcevic G, Koutsouris A, Tripuraneni J, Lorimer DD, Nowak G, Guerriero V Jr, Elson EL, Lanerolle PD. 1996. Expression of the catalytic domain of myosin light chain kinase increases paracellular permeability. Am J Physiol. 271(5 Pt 1):C1678–C1684.

Honda M, Nakagawa S, Hayashi K, Kitagawa N, Tsutsumi K, Nagata I, Niwa M. 2006. Adrenomedullin improves the blood-brain barrier function through the expression of claudin-5. Cell Mol Neurobiol. 26(2):109–118.

Kilkenny C, Browne W, Cuthill IC, Emerson M, Altman DG. 2010. Animal research: reporting in vivo experiments. The ARRIVE guidelines. Br J Pharmacol. 160(7):1577–1579.

Kluger MS, Clark PR, Tellides G, Gerke V, Pober JS. 2013. Claudin-5 controls intercellular barriers of human dermal microvascular but not human umbilical vein endothelial cells. Arterioscler Thromb Vasc Biol. 33(3):489–500.

Lemp MA, Baudouin C, Baum J, Dogru M, Foulks GN, Kinoshita S, Laibson P, McCulley J, Murube J, Pflugfelder SC, et al. 2007. The definition and classification of dry eye disease: report of the definition and classification subcommittee of the international dry eye workshop. Ocul Surf. 5(2):75–92.

Masedunskas A, Milberg O, Porat-Shliom N, Sramkova M, Wigand T, Amornphimoltham P, Weigert R. 2012. Intravital microscopy: a practical guide on imaging intracellular structures in live animals. Bioarchitecture. 2(5):143–157.

Melvin JE, Yule D, Shuttleworth T, Begenisich T. 2005. Regulation of fluid and electrolyte secretion in salivary gland acinar cells. Annu Rev Physiol. 67:445–469.

Nitta T, Hata M, Gotoh S, Seo Y, Sasaki H, Hashimoto N, Furuse M, Tsukita S. 2003. Size-selective loosening of the blood-brain barrier in claudin-5-deficient mice. J Cell Biol. 161(3):653–660.

Peppi M, Ghabriel MN. 2004. Tissue-specific expression of the tight junction proteins claudins and occludin in the rat salivary glands. J Anat. 205(4):257–266.

Plumb J, McQuaid S, Mirakhur M, Kirk J. 2002. Abnormal endothelial tight junctions in active lesions and normal-appearing white matter in multiple sclerosis. Brain Pathol. 12(2):154–169.

Roy S, Kim D, Hernández C, Simó R, Roy S. 2015. Beneficial effects of fenofibric acid on overexpression of extracellular matrix components, COX-2, and impairment of endothelial permeability associated with diabetic retinopathy. Exp Eye Res. 140:124–129.

Shen L, Black ED, Witkowski ED, Lencer WI, Guerriero V, Schneeberger EE, Turner JR. 2006. Myosin light chain phosphorylation regulates barrier function by remodeling tight junction structure. J Cell Sci. 119(Pt 10):2095–2106.

Shi S, Verin AD, Schaphorst KL, Gilbert-McClain LI, Patterson CE, Irwin RP, Natarajan V, Garcia JG. 1998. Role of tyrosine phosphorylation in thrombin-induced endothelial cell contraction and barrier function. Endothelium. 6(2):153–171.

Tsukita S, Furuse M, Itoh M. 2001. Multifunctional strands in tight junctions. Nat Rev Mol Cell Biol. 2(4):285–293.

Wang J, Li C, Chen T, Fang Y, Shi X, Pang T, Zhang L, Liao H. 2016. Nafamostat mesilate protects against acute cerebral ischemia via blood-brain barrier protection. Neuropharmacology. 105:398–410.

Yang C, DeMars KM, Hawkins KE, Candelario-Jalil E. 2016. Adropin reduces paracellular permeability of rat brain endothelial cells exposed to ischemia-like conditions. Peptides. 81:29–37.

Yang H, Yu PK, Cringle SJ, Sun X, Yu DY. 2015. Intracellular cytoskeleton and junction proteins of endothelial cells in the porcine iris microvasculature. Exp Eye Res. 140:106–116.

Yu GY, Zhu ZH, Mao C, Cai ZG, Zou LH, Lu L, Zhang L, Peng X, Li N, Huang Z. 2004. Microvascular autologous submandibular gland transfer in severe cases of keratoconjunctivitis sicca. Int J Oral Maxillofac Surg. 33(3):235–239.

Zhang LW, Cong X, Zhang Y, Wei T, Su YC, Serrão AC, Brito AR Jr, Yu GY, Hua H, Wu LL. 2016. Interleukin-17 impairs salivary tight junction integrity in Sjögren's syndrome. J Dent Res. 95(7):784–792.